**Proceedings of the 8th International Conference on MicroManufacturing**
**University of Victoria, Victoria, BC, Canada, March 25-28, 2013**

# Micro Injection Molded Microtopographic Polymer Plates used to Mechanically Direct Stem Cell Activity

ICOMM
2013
**No. 9**

John W. Rodgers[1], Meghan E. Casey[2], Sabrina S. Jedlicka[3], and John P. Coulter[4]
[1]Mechanical Engineering and Mechanics; Lehigh University; Bethlehem, PA; John.Rodgers@lehigh.edu
[2]Bioengineering; Lehigh University; Bethlehem, PA; mec411@lehigh.edu
[3]Materials Science and Engineering, Bioengineering, Center for Advanced Materials and Nanotechnology; Lehigh University; Bethlehem, PA; ssj207@lehigh.edu
[4]Mechanical Engineering and Mechanics; Lehigh University; Bethlehem, PA; e-mail: jc0i@lehigh.edu

## ABSTRACT

A novel micro injection molding assembly which allows for firm yet compliant housing of silicon tooling was designed and manufactured. Microchannels were etched into a silicon wafer through the use of ultraviolet lithography (UVL) combined with deep reactive ion etching (DRIE). Injection molded polystyrene plates containing microtopography were fabricated in which multiple molding parameter studies were executed to further understand the effect of mold temperature and injection velocity on replication. Micro and nano featured polymeric substrates have tremendous potential for use in stem cell culture, as cells are exposed to and controlled by microtopography in their natural environment.

## INTRODUCTION

Micro injection molding can be used to manufacture macroscale parts containing microtopography. During conventional injection molding, a molten polymer liquid enters and fills a pre-machined cavity and freezes upon contact with the cooler mold walls. The immediate frozen layer would be a fatal flaw if attempting to fill microfeatures present at the cavity surfaces. Consequently, mold temperatures are typically maintained around glass transition temperature to provide adequate mobility of the polymer chains to fill channels prior to freezing [1]. Increases in injection velocity and melt temperatures also have been shown to enhance replication [2,3]. At certain size scales, traditional machining of the mold cavity becomes impossible and alternate methods must be used. Techniques derived from the electronics industry can be implemented to create micro and nanofeatured substrates. One such technique is UVL, in which a 2 dimensional geometric pattern is projected onto a photosensitive substrate via the combination of a selectively light permeable mask and ultraviolet rays. The material most commonly used for lithography is silicon. UVL is followed by etching (wet or dry) to permanently transfer the geometry to the silicon wafer. To fabricate anisotropic features, DRIE, which is a dry etching process, can be used. By using UVL with DRIE, a large area of microchannels can be fabricated over a relatively large surface area.

Silicon has been used in multiple studies as a microfeatured tooling material for injection molding. It is often considered to be used more for prototyping than for industrial mold assemblies due to its brittle nature, with metal stampers being a more durable alternative [4]. However, the robustness of silicon tooling over a period of a relatively large number of cycles has been proven as well [5].

Molded macroscale polymer parts containing micro and nanotopography have previously been used for the purpose of inducing specific stem cell responses in a cell culture laboratory environment. Microfeatured polymer plates have also been used to differentiate stem cells into particular cell types and as a means to prevent stem cells from differentiating [6,7]. However, a very limited number of studies have used the high throughput manufacturing process of injection molding, to fabricate such substrates [8,9]. In addition to topography, it has been shown that stem cell differentiation can be controlled by substrate stiffness, in which stiffness values equivalent to a particular biological tissue type will cause stem cells to begin differentiating into the same cell type [10].

Polystyrene (PS), a relatively stiff thermoplastic, is the polymer used to make the standard cell culture dish used in laboratories worldwide. Although biocompatible with proper plasma treatment, the stiffness of PS is multiple orders of magnitude greater than that of biological tissue. To avoid using a different material, it is hypothesized that a locally more compliant surface stiffness can be created through the use of molded microfeatures capable of elastically deforming.

Classical mechanics can be used to determine the optimal cross-sectional shape of a beam to be used that would result in the most significant reduction in apparent stiffness. The area moment of inertia is a measurement of the resistance to bending of a beam. To obtain a low apparent stiffness, the inertia must therefore be minimized, in which the value is determined through the integral:

$$I = \iint y^2 \, dA \qquad (1)$$

The value "y" is the distance from the axis of rotation and the cross-sectional area. Consequently, a circular cross-section satisfies this requirement, and cylindrical beams are

chosen as the stiffness reduction geometry. According to the Euler-Bernoulli beam bending approximation, the deflection is given by:

$$\upsilon = 64FL^3 / 3\pi ED^4 \quad (2)$$

*F* is a force applied at the tip of the beam, *L* is the length of the beam, *E* is the bulk modulus of the material, and *D* is the diameter of the pillar. It is hypothesized that if the cell comes into contact with the deflecting micropillars (instead of bulk PS) that the mechanical perception of the substrate from a cellular processing perspective will be a more compliant substrate.

The current study focuses on the manufacturability of such stiffness reducing microfeatured substrates, and specifically the filling behavior of a micro injection molded network of polystyrene pillars.

## EXPERIMENTAL

### *A. UV PHOTOLITHOGRAPHY*

A 1564 Å thick layer of silicon dioxide was deposited onto the surface of a P-type Crysteco 3 inch silicon wafer with a thickness of 509 ± 26 µm. OCG 825 positive photoresist was spin coated at 5,000 rpms for 40 s onto the wafer, yielding a layer of 9000 Å. A photolithography mask containing transparent holes orthogonally arrayed with a diameter of 2 µm and spacing of 3 and 4 µm was placed over top of the coated wafer, and UV exposure was applied using a Karl Suss MJB3 mask aligner at a power of 25 W for 1.4 s. The wafer was immersed in an OCG 809 solution for 20 s (photoresist developer), and rinsed with water, leaving regions of exposed silicon dioxide ($SiO_2$). To remove the $SiO_2$ and expose silicon in preparation for etching, the wafer was submerged in buffered HF for a period of 7 min.

The Bosch process was used, in which activation and passivation gases were plasma polymerized for a prescribed number of cycles. The etching conditions are shown in *Table 1*. Each cycle consisted of a 3 s period of sulfur hexafluoride ($SF_6$), which etches isotropically, and a 2 s period of octafluorocyclobutane ($C_4F_8$), which provides a protective coating to the sidewalls of the microchannel (allowing for a net anisotropic feature). The wafer was then immersed in photoresist stripper to reveal bare silicon. A final deposition of $C_4F_8$ was applied as an anti-stiction agent. *Fig. 1b* shows a schematic of the etched profile that is created from the process.

### *B. MOLD ASSEMBLY*

The silicon wafer was diced into 10 x 10 $mm^2$ squares and inserted into the mold assembly (*Fig. 1*), in which the wafer sits inside of an aluminum backing that is screwed into the aluminum insert. When screwed in, the wafer occupies a square window present in the aluminum insert. A 0.02'' thick layer of PTFE was positioned between the wafer and wafer backing to dampen the impact load of the polymer during molding. A 0.01'' thick PTFE gasket was fixed in front of the wafer to provide a mechanical buffer between aluminum and silicon, and to seal off the cavity. The main mold cavity includes a sprue, cold slug well, short runner, and fan gate. The type of gate was chosen to provide a uniform flow front across the part and presumably impart an equal filling of microcavities. The resultant macroscale molded part was a plate with a raised platform containing the microtopography (*Fig. 3*). Two cartridge heaters on either side of the mold which were used to heat the assembly, combined with wire thermocouples, provided a closed-loop feedback control to maintain specific mold temperatures throughout the molding process.

***Table 1: DRIE Conditions used to create microchannels.***

| Plasma Type | flow (SCCM) | time /cycle (s) | Source Power (W) | Cycles | Processing time |
|---|---|---|---|---|---|
| $SF_6$ | 125 | 3 | 1200 | 34 | 2 m 50 s |
| $C_4F_8$ | 100 | 2 | 1200 | | |
| $C_4F_8$ | 150 | 20 | 1500 | 1 | 20 s |

### *C. MICRO INJECTION MOLDING*

Micro injection molding trials were conducted with a 3 ton 2 stage injection unit micro injection molding machine (Nissei AU3E). The polymer molded was general purpose polystyrene (666D, Americas Styrenics$^{LLC}$).

The polymer has a melt flow rate of 8 g/10 min (200 $^oC$ / 5 kg; D-1238), elastic modulus of 3,000 ± 34 MPa, and Vicat Softening Temperature of 99 $^oC$. Polystyrene was chosen due to its widespread use as a cell culture platform in the laboratory. A study on the effect of lower mold temperatures ($<T_g$) was executed to analyze the progression of the melt flow into microchannels (trial 1).

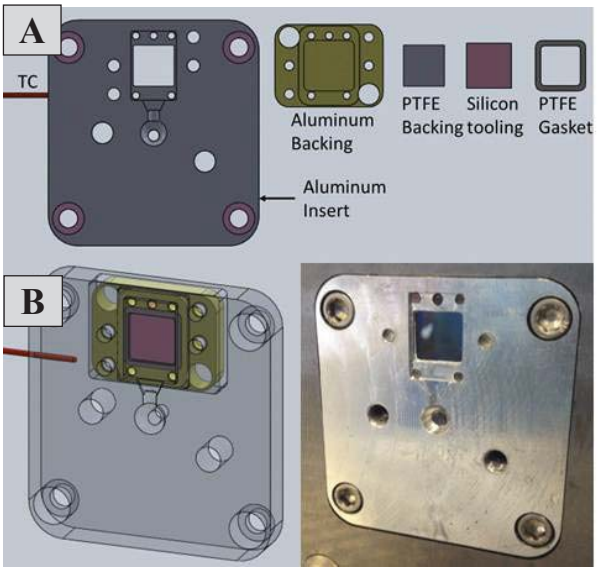


***Fig. 1: Micromold Aluminum insert assembly exploded (A) and assembled (B). TC = thermocouple.***

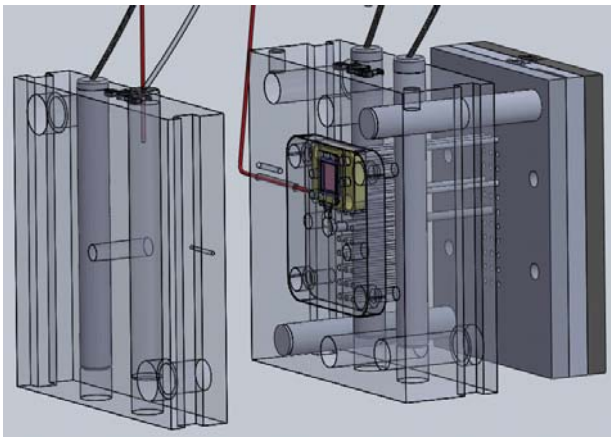

*Fig. 2: Full mold assembly schematic. The red rods are wire thermocouples.*

In addition, a study analyzing the effect of injection velocity on replication was conducted at mold temperatures above the $T_g$ of polystyrene (which is assumed to be 91 $^oC$, trial 2). The molding conditions for trial 1 are shown in Table 2. The injection time (filling time + holding time) was maintained at 8 s, cooling time was held constant at 20 s, holding pressure was 19.3 MPa, and back pressure was 4.1 MPa for both trials. The temperature zones were set to 232.2 $^oC$ / 226.7 $^oC$ / 226.7 $^oC$ / 221.1 $^oC$ / 201.7 $^oC$ from the nozzle to the rear of the plastication screw, respectively. For trial 2, injection flow was the test parameter (Table 3). To further facilitate microfeature filling, the barrel temperatures were increased. Injection time was 8 s, cooling time was dictated by the mold temperature reaching 82.2 $^oC$, and holding and back pressures were the same as trial 1. Temperature zones were 248.9 $^oC$ / 243.3 $^oC$ / 232.2 $^oC$ / 221.1 $^oC$ / 201.7 $^oC$ for trial 2. Melt temperature, or the temperature of the polymer as it leaves the injection unit, was measured using the "30-30-30 rule" with a wire thermocouple (30 cycles, 30$^oC$ above predicted temperature, 30 s wait prior to measurement). A LEO 1550 Variable Pressure Scanning Electron Microscope was used to image the surface of the wafer and polymer samples in distinct regions of the part. For trial 1, images were taken near the gate. For trial 2, 9 distinct locations on the surface of the part were recorded (shown in Fig. *3*). When measuring pillar height as a function of the distance from the gate, the middle regions (2, 5, and 8) were used.

***Table 2: Molding conditions for Trial 1***

| Specimen # | $T_{mold}$ ($^oC$) | Flow Rate, Q ($cm^3/s$) |
|---|---|---|
| 1a | 65.6 | 7.54 |
| 1b | 76.7 | 2.51 |
| 1c | 76.7 | 5.03 |
| 1d | 76.7 | 7.54 |

***Table 3: Molding conditions for Trial 2***

| Specimen # | Flow Rate, Q ($cm^3/s$) |
|---|---|
| 2a | 2.01 |
| 2b | 4.02 |
| 2c | 6.03 |

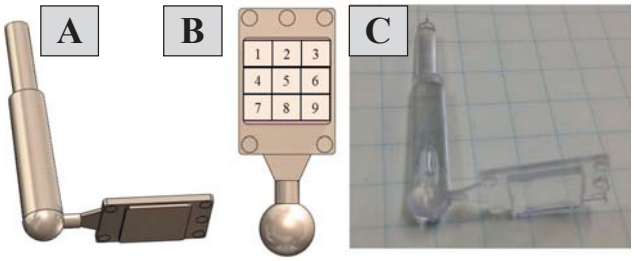


*Fig. 3: Schematic of molded part (A), locations of measured regions (B) and actual molded part (C).*

## RESULTS AND DISCUSSION

UVL with DRIE yielded microchannels on the surface of the silicon wafer. (*Fig. 4*). There is a widening near the top of the channel. Presumably, photoresist protected the top edge of the holes for a majority of the etch time and eventually was etched away, allowing for an increase in diameter near the channel entrance.

The microchannels had a diameter of 1.64 μm and depth of 4.75 μm, which corresponds to an etch rate of 1.68 μm/min and aspect ratio of 2.9 (***Table 1***). The channels appear to be straight, with sidewall scallops (an inherent result of the Bosch process). The etch rate is dependent on many different parameters, such as plasma flow rate, wafer temperature, and activation to passivation ratio.

One common concern associated with injection molding is the presence of undercuts in the tooling cavity. Undercuts lead to damage of the molded part, causing final part deformation as well as residual polymer inside the cavity. In fact, it is recommended that some draft be on all positive part features to ensure proper part ejection. A draft angle was intentionally avoided due to the specific geometrical design requirements of a cylindrical beam with constant cross-section.

The scallops imparted to the sidewalls during the etching process can be considered nano-undercuts that could potentially hinder the ejection of the micropillars. Nevertheless, a taper near the top of the of cavity provides facilitation of ejection and a slightly increased mechanical stability for the molded pillars.When molding using mold temperatures below $T_g$, replication values are dramatically reduced, as premature solidification occurs prior to filling the microcavities.

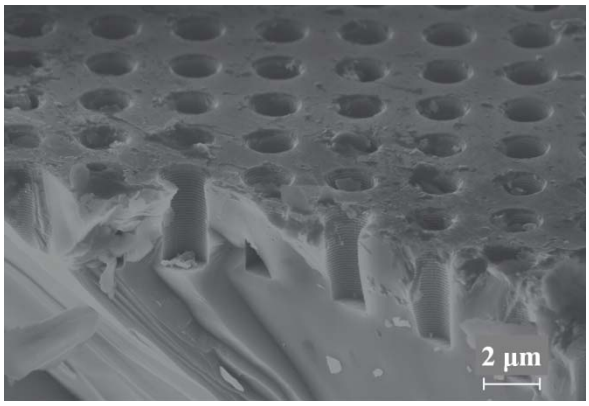


*Fig. 4: Microfeatured silicon mold insert micrograph and microchannel dimensions.*

*Table 4: Microchannel dimensions*

| Dimensions | 3 µm C2C |
|---|---|
| Depth | 4.75 ± .08 µm |
| $Diameter_{channel}$ | 1.64 ± .03 µm |
| $Diameter_{top}$ | 1.84 ± .02 µm |

Near the gate, an increase in mold temperature from 65.6 °C to 76.7 °C allows for minimal flow into the cavity, as evidenced by Fig. 5B. A common behavior associated with injection molding is hesitation flow, in which the polymer fills larger regions of a cavity prior to the smaller domains. The delayed filling of the microcavities allows the polymer near the wall to cool for an additional period of time, thereby increasing its viscosity.Viscosity, defined as the resistance of fluid to flow, is a function of shear rate, temperature, and pressure. It is often modeled through the use of the cross-WLF equation, in which viscosity is shown to decrease with increasing shear rate and increasing melt temperature since it is a non-Newtonian fluid (*Fig. 6*, constants for polystyrene obtained from Autodesk® Moldflow database).

$$\eta_{bulk} = \eta_o / ((1+(\eta_o/\tau))^{(1-n)}) \quad \textbf{(3)}$$

ηbulk is the bulk viscoity of the polymer, η0 is the viscosity at a zero shear rate, and is determined through a calculation performed with experimentally determined constants. Viscosity tends to follow such trends in a linear manner (in a logarithmic scale) above a certain shear rate threshold, and appears to do so independent of melt temperature (see *Fig. 7*). At at a shear rate of 100 $s^{-1}$, a 176 °C reduction in temperature only increases the viscosity by 22 Pa*s, compared to a 2928 Pa*s increase in viscosity with the identical temperature difference at a shear rate of 1 $s^{-1}$. Hesitation flow allows for a decrease in shear rate, therefore making the microchannel flow susceptible to polymer viscosity which is highly sensitive to the melt temperature.

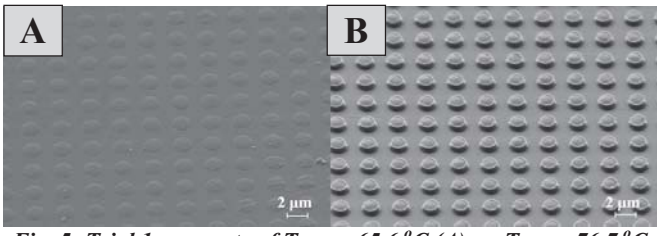


*Fig. 5: Trial 1 near gate of $T_{mold}$ = 65.6 °C (A) vs. $T_{mold}$ = 76.7 °C at identical flow rate of 7.54 $cm^3/s$.*

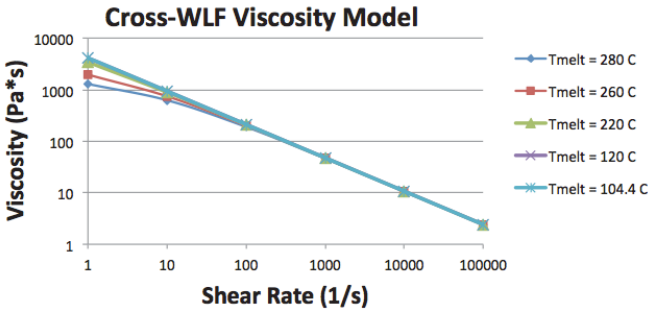


*Fig. 6: Cross-WLF plot of Viscosity vs. Shear Rate for different melt temperatures of 666D.*

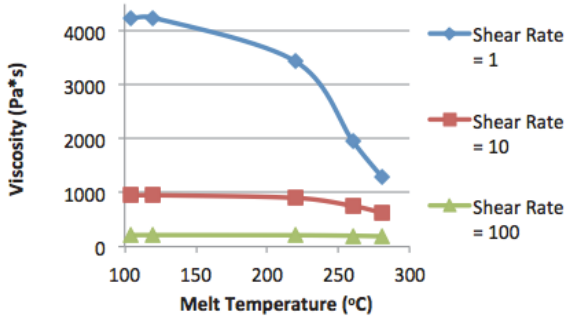


*Fig. 7: Viscosity vs. Melt temperature at different shear rates.*

Injection velocity was also varied at a constant mold temperature of 76.7 °C. Replication remained relatively constant even when comparing the lowest and highest flow rates (which differ by a factor of 3) (*Fig. 8*). It is quite apparent that although some degree of microchannel filling can occur with a mold temperature below $T_g$ of the polymer being molded, the achievable replication is fairly low, and is very difficult to enhance even when altering parameters known to affect replication (such as flow rate).

Increasing the mold temperature, although a positive influence for replication, often leads to additional processing time, and may impart deleterious defects such as lower molecular weight and increased brittle behavior. The additional process time is accredited to the mold being above ejection temperature of the polymer, in which the molded part is too hot to allow for ejection. A "variotherm" system is required to increase and reduce mold temperature synchronously with the molding cycle. An effective variotherm process does not sacrifice cycle time.

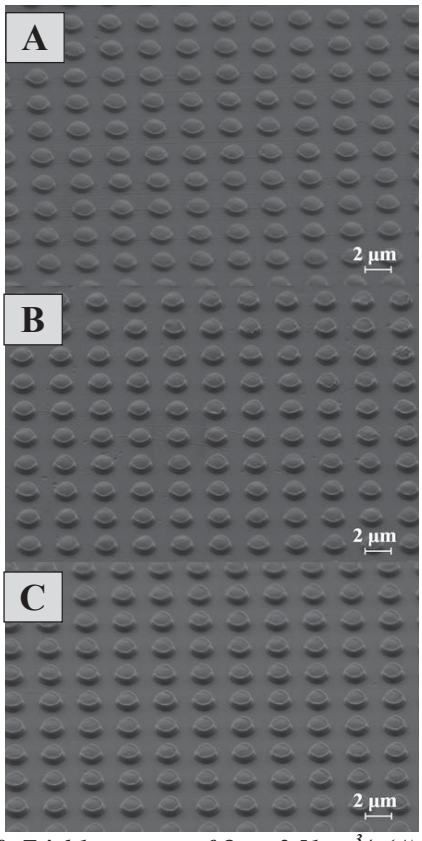


***Fig. 8: Trial 1 near gate of $Q_{inj}$ = 2.51 $cm^3/s$ (A), 5.03 $cm^3/s$ (B), and 7.54 $cm^3/s$ (C).***

However, it does result in increased wear of the tooling as a result of rapid heating and cooling [11].The second trial imparts such a system, in which the tooling is actively heated and passively cooled.

In trial 2, the mold temperature was maintained well above the $T_g$ of 666D, with polymer flow rate during the filling phase being the varied parameter. The set barrel and screw conditions led to a melt temperature of 196.1 $^oC$. SEM micrographs were collected in 9 different regions to provide a comprehensive view of the filling activity across the part (*Fig. 9*, *Fig. 10*, *Fig. 11*). With a few exceptions, measured pillar heights were greater than that of samples molded at mold temperatures below $T_g$ of polystyrene. The few areas where replication is poor is most likely due to the presence of micro sink marks, in which the warmer polymer below the surface has pulled the pillar surface towards the core of the part.

The highest replication occurred near the gate for all three flow rates. Replication is defined here as the ratio of pillar height to microcavity depth. For the lowest flow rate (*Fig. 9*), the highest achievable replication was 0.257 (pillar height = 1.22 ± 0.05 µm). The middle flow rate yielded a height replication value of 0.267 and the high flow rate resulted in a maximum value of 0.609.

Increasing the flow rate by a factor of even 2 significantly enhanced replication when the mold temperature was maintained above $T_g$ during the filling and compensation phases of the molding cycle, as shown in *Fig. 9* and *Fig. 10*. For the part molded with a flow rate of 2.01 $cm^3/s$, pillars are barely visible for both the end of fill and middle region. In contrast, pillars are beginning to form in the same locations for the part molded at 4.02 $cm^3/s$. The highest level of replication was achieved through using the highest flow rate. However, the consistency of pillar height across the part was greatest for the middle flow rate.

The top surface of the pillars appear to be concave for those with lesser height, in which the middle of the surface is slightly collapsed. The uneven surface could be due to the presence of trapped air inside of the cavity. Traditionally injection molding involves venting of air from the tooling cavity through either shallow channels which run along the tooling surface or through the clearance between the ejector pins and ejector pin holes. However, designs which include microcavities with relatively high aspect ratios create a situation where the air has no avenue to escape and thus becomes trapped inside the microfeatures. When attempting to fill the cavity, the air pushes against the polymer melt and prevents further filling from occurring. Moreover, the air may push in a radial direction, causing the concave feature on the pillar surface. Vacuum venting has been suggested as a potential solution to the trapped air dilemma. However, designing and implement such systems is rather costly and has proven only marginally successful.

Another potential cause for the pillar tip shape is the presence of a micro sink mark, in which the core of the pillar is insulated from the relatively cooler walls of the microcavity. When the hotter internal polymer cools, it contracts and can pull the solidified polymer down into the center of the feature.

The uneven pillar tips could also be due to a locally lower viscosity at the microcavity tooling surface. The nanoridges present on microcavity walls may enhance the shear thinning effect, as the melt is subjected to a certain nanoroughness along the wall. It would be interesting to note whether the same surface geometry occurred at a smaller scale. It has been previously suggested by Yao *et al*. that as feature dimensions are reduced, the lower viscosity regions of an advancing flow front transition from the outer region (where higher shear rates are present) to the center of the flow [12].

The consideration of microscale viscosity can be made within the context of the Cross-WLF model, in which such value is given as:

$$\eta_{micro} = (\gamma dot, T, P) = (1+ \xi(g^2/z^2))* \eta_{bulk} \quad (4)$$

$\xi$ is a non-dimensional constant specific to the polymer being molded, g is the radius of gyration of the polymer molecular chain, and z is the thickness of the polymer fill region. The locally higher viscosity is attributed to molecular effects near the wall, in which the forces associated with molecular bonds are no longer negligible, but begin to contribute to the resistance to movement of the polymer.

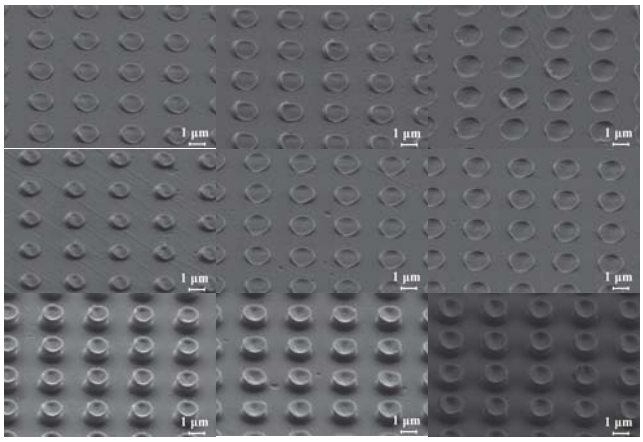

*Fig. 9: Micrographs of 9 regions of PS molded with flow rate of 2.01 cm$^3$/s.*

Molecular effects have also been suggested as a cause for increased elastic modulus with decreasing scale [13].

For the pillars with the highest replication, the tip concavity is relatively reduced. The presence of taller pillars indicate that the flow length inside of the microchannel increased. As the polymer flows through the channel, it is most likely the case that the flow path narrows as the polymer is filling.Consequently, a local microscale flow regime can occur, in which the solidified polymer essentially functions as a part of the mold cavity. Resultantly, the microscale flow phenomenon of lower viscosity towards the middle of the channel could provide enhanced filling capacity away from the wall and thus decrease the concave features present on the lesser filled microchannels.

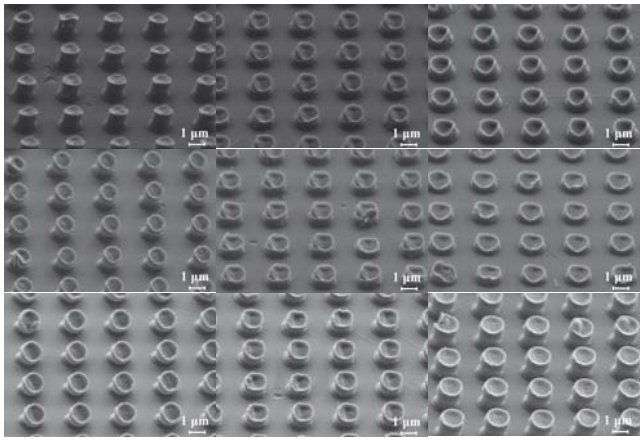

*Fig. 10: Micrographs of 9 regions of PS molded with flow rate of 4.02 cm$^3$/s.*

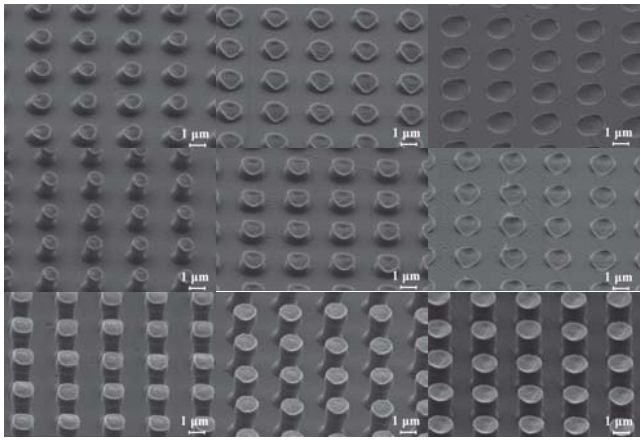

*Fig. 11: Micrographs of 9 regions of PS molded with flow rate of 6.03 cm$^3$/s.*

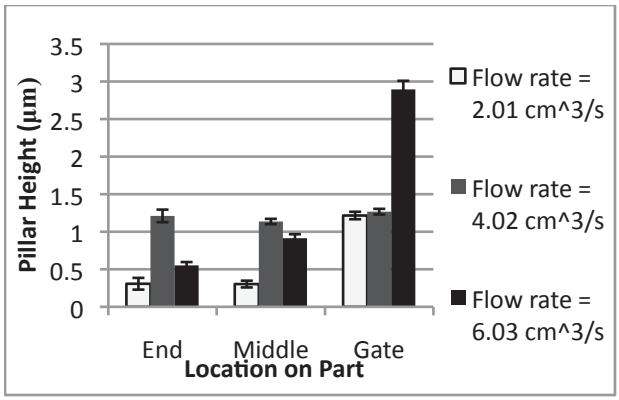


*Fig. 12: Pillar heights along the part for different flow rates at a mold temperature of 104.4 $^o$C.*

One consideration previously mentioned is the need for a taper on negative tooling (i.e., positive featured parts). The scallops present on the sidewalls of the silicon tooling are seen as witness marks on the sides of the pillars. There also appears to be a slight stretching of the pillars occurring in response the interaction between the pillars and silicon scallops (Fig. *13*).

## CONCLUSION

Polystyrene substrates containing polymer microtopography were fabricated using the high throughput high precision manufacturing method of micro injection molding. Mold temperature and injection velocity were both shown to alter replication of the microfeatures. Moreover, the scallops present on the sides of the microcavities were shown to alter the geometry of microfeatures.

Further design and experimentation will be executed within the context of traditional injection molding principles (slight draft angles on microfeatures) combined with novel micro and nanoscale processing considerations (microscale viscosity, size scale dependence of elastic modulus) to move closer to achieving a highly uniform network of microfeatures for use in mechanically directing the activity of stem cells.

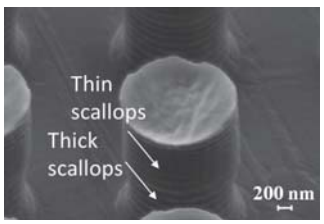


*Fig. 13: Micrograph of pillars with slightly stretched scallop marks closer to base of pillar.*

Acknowledgements: National Science Foundation (Grant #1014987), Ray Filozof, Bill Mushock, Brian Slocum for laser cut gaskets.

## REFERENCES

[1] M. Heckele, "Review on micro molding of thermoplastic polymers," *Journal of Micromechanics and Microengineering*, 2004; 14: R1-R14.

[2] B. Sha, "Investigation of micro-injection moulding: Factors affecting the replication quality," *Journal of Materials and Processing Technology*, 2007; 183: 284-296.

[3] C. Srirojpinyo, "Processing Parameters Affecting Nanoinjection Molding," *NSTI-Nanotech.* 2004: 464-467.

[4] N. Zhang, "Replication of micro/nano-scale features by micro injection molding with a bulk metallic glass insert," *Journal of Micromechanics and Microengineering*, 2012; 22: 065019.

[5] S.H. Yoon. "Evaluation of novel tooling for nanoscale injection molding," *SPIE International Symposia, Smart Structures & Materials / NDE*; San Diego, 2005. 107-116.

[6] M. Mrksich, "Stem Cell Differentiation: Multipotency retained," *Nature Materials*, 2011; 10:559-560.

[7] J. Fu, "Mechanical regulation of cell function with geometrically modulated elastomeric substrates," *Nature Methods*, 2010; 7: 733-736.

[8] C. Holzer, "Nanostructured polymer surfaces to optimize cell behavior. ANTEC. Orlando, FL: Society of Plastics Engineers. 2012.

[9] N. Gadegaard,"Biomimetic Polymer Nanostructures by Injection Molding," *Macromolecular Materials and Engineering*, 2003; 288: 76-83.

[10] Y Pek, "The effect of matrix stiffness on mesenchymal stem cell differentiation in a 3D Thixotropic gel," *Biomaterials*, 2010; 31:385-391.

[11] J. Giboz, "Microinjection molding of thermoplastic polymers: a review," Journal of Micromechanics and Microengineering, 2007; 17: R96-R109.a

[12] D. Yao, "Simulation of the filling process in micro channels for polymeric materials," *Journal of Micromechanics and Microengineering*, 2002;12: 604-610.

[13] L. Sun. "Modeling the size-dependent elastic properties of polymeric nanofibers," *Nanotechnology*, 2008; 19: 455706-455713.